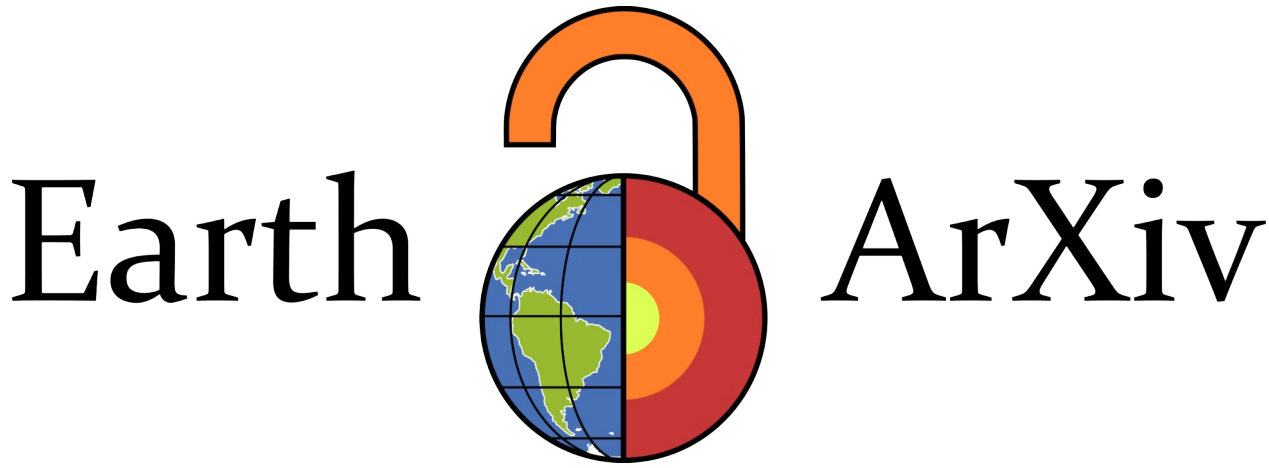

Storm life cycle modulates extreme hydroclimate impact risk: a Great Lakes Region case study

D. C. Jones[1], J. Ward[2], A. Hutson[1], L. Ru[1], D. M. Wright[3], A. H. Young[3], L. M. Fry[3]

[1]Cooperative Institute for Great Lakes Research, University of Michigan
[2]US Army Corps of Engineers - Detroit District
[3]NOAA Great Lakes Environmental Research Laboratory

Key Points:

- Storm life-cycle state at Great Lakes entry organizes the risk of extreme extra-tropical cyclone impacts
- Extreme evaporation risk is systematically higher in Fall (SON) for storms that enter the region later in their life cycle
- Extreme precipitation risk is also elevated for later-entry storms, with the clearest signals emerging in summer in the upper Great Lakes

Corresponding author: D. C. Jones, dannes@umich.edu

Abstract

Extratropical cyclones (ETCs) drive hydroclimate variability in the Great Lakes, yet their impacts vary widely between events. Here, we classify ETCs into two storm types using an unsupervised clustering approach based on storm properties and evolution. The resulting classes differ systematically in life cycle stage at Great Lakes entry. Using bootstrap-estimated risk ratios and risk differences, we show that storms entering later in their life cycle have a higher risk of extreme evaporation during autumn (SON) across all five lakes. In contrast, precipitation responses are weaker, more spatially heterogeneous, and most evident in summer over the upper lakes. Differences in storm genesis location do not fully explain these patterns, indicating that storm evolution at interaction provides a more informative organizing axis. These results demonstrate that storm life cycle stage governs the risk of extreme lake–atmosphere fluxes and offer a transferable framework for storm-centric impact assessment.

Plain Language Summary

Large storms called extratropical cyclones are a major driver of extreme weather in the Great Lakes, but their impacts vary widely from storm to storm. In this study, we show that storms can be grouped into two main types based on when they reach the Great Lakes during their life cycle. Storms that arrive later in their development are more likely to produce extreme evaporation during the fall, increasing the likelihood of these events across all five lakes.

Differences in extreme precipitation are weaker and less consistent. The clearest rainfall signals appear during summer in the upper Great Lakes, while other regions show little systematic difference between storm types. We also find that the two storm types tend to form in different locations, with later-developing storms forming farther west.

Overall, our results show that how a storm evolves plays an important role in shaping extreme weather risks in the Great Lakes. Because large lakes interact with storms in similar ways around the world, this approach may also help assess extreme weather risks in other regions.

1 Introduction

Large lake regions are tightly coupled lake–atmosphere systems that are sensitive to hydroclimate variability, particularly precipitation and evaporation (Anyah & Semazzi, 2009; Notaro et al., 2013; Raible et al., 2021; Kunkel et al., 2022). Evaporation from large lakes can strongly influence downstream weather, including lake-effect precipitation. This process is pronounced in the North American Great Lakes, where relatively warm lake temperatures enhance moisture availability and modify near-surface atmospheric conditions, with impacts on local and regional weather (Scott & Huff, 1996; Angel & Isard, 1997; Vavrus et al., 2013; Wang et al., 2022). These interactions can extend beyond the lakes themselves, influencing regional climate variability and extremes across broad spatial scales (Hawcroft et al., 2012; Xiao et al., 2018; J. Hanrahan et al., 2021; Clare et al., 2023).

The Laurentian Great Lakes are a large, interconnected freshwater system that provides a well-observed testbed for studying hydroclimate variability. Lake levels are sensitive to imbalances among precipitation, runoff, and evaporation (Quinn, 2009; J. L. Hanrahan et al., 2010; Gronewold et al., 2016). Despite a relatively dense observational network, evaporation remains poorly constrained and is often inferred from models or reanalysis products. Extreme evaporation events play an important role by enhancing heat and moisture exchange, driving lake-effect precipitation, and contributing to lake level variability, with direct implications for infrastructure, navigation, water supply, and flood risk (Neff & Nicholas, 2005).

Extratropical cyclones (ETCs) are a dominant driver of hydroclimate extremes in the GLR, including changes in precipitation intensity and frequency (Angel & Isard, 1998; Hawcroft et al., 2012; Raible et al., 2021). These synoptic-scale systems account for a large fraction of extreme precipitation events and are central to assessments of hydroclimate risk and water resource management (Pfahl & Wernli, 2012; Kunkel et al., 2022). Changes in storm tracks and large-scale circulation are expected to modify ETC behavior, with implications for precipitation extremes (Angel & Kunkel, 2010; Hawcroft et al., 2012; Raible et al., 2021). Observations indicate shifts in the spatial distribution of ETC activity, including northward shifts affecting the Great Lakes (Hutson et al., 2024), with clear seasonal structure (Chang et al., 2016; Gertler & O'Gorman, 2019; Fritzen et al., 2021).

ETCs evolve through distinct life cycle stages, with each stage associated with different dynamical and thermodynamic characteristics (Booth et al., 2018). The mature phase is typically associated with strong winds, enhanced moisture transport, and well-developed frontal structure, all of which influence precipitation and air–lake fluxes. Interaction with large lakes during this stage can amplify local and downstream impacts (Anyah & Semazzi, 2009). As a result, storm evolution plays a central role in shaping hydroclimate impacts.

Despite this, the relationship between storm evolution and impacts on large lake systems remains poorly resolved. Many studies relate ETC frequency or intensity to precipitation and evaporation without accounting for life cycle stage, implicitly treating storms as temporally uniform (Agustí-Panareda et al., 2005; Eichler & Higgins, 2006; Fritzen et al., 2021; Hutson et al., 2024). Conversely, studies of storm evolution rarely link structure directly to lake-specific impacts. Classification approaches based on storm origin or track provide useful context but do not fully explain variability in downstream impacts (Riemer & Jones, 2010). As a result, the connection between storm life cycle state and extreme lake impacts remains largely unquantified.

In this study, we take a storm-centric, Lagrangian approach to linking extratropical cyclone (ETC) evolution with extreme lake impacts using the Great Lakes as a testbed. We analyze an event-resolved dataset pairing storm characteristics with lake-specific pre-

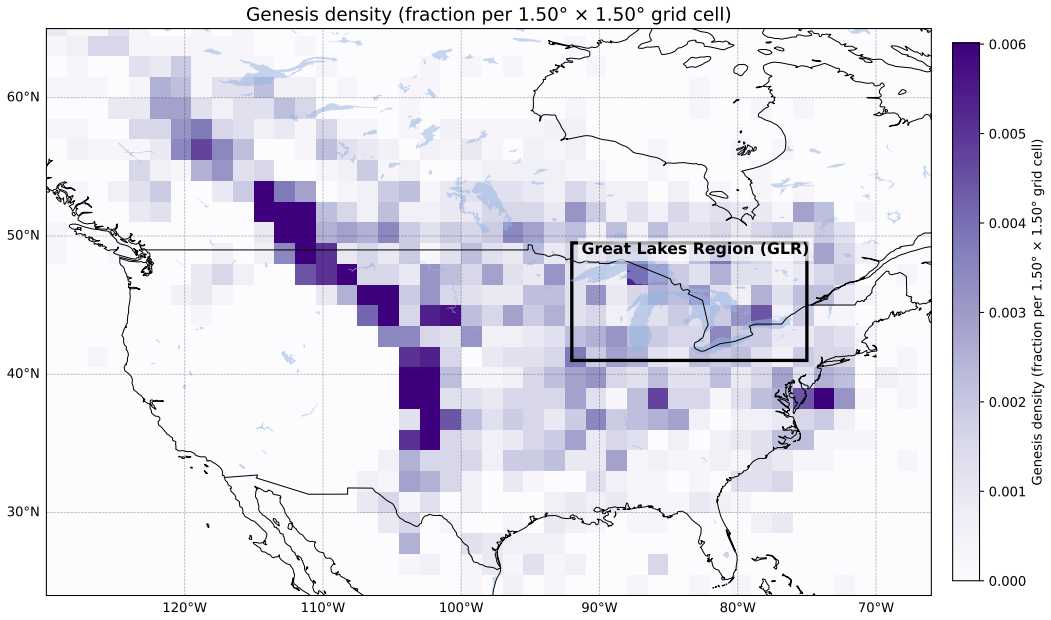

Figure 1. Heatmap of extratropical cyclone genesis from the CFSR dataset (1979–2019), expressed as the fraction of storms per 1.5° grid cell. The Great Lakes Region (GLR) is outlined in black.

cipitation and evaporation impacts. Using unsupervised classification, we allow storm evolution to emerge as an organizing feature without prescribing categories. We focus on simple proxies for storm maturity and residence time within the Great Lakes Region (GLR), providing a coarse representation of storm evolution during lake interaction. While simplified, these metrics enable us to assess whether storm evolution organizes the risk of extreme hydroclimate impacts. The framework is transferable to other large lakes, inland seas, and regions influenced by ETC-driven extremes.

2 The extratropical cyclone impacts dataset

To examine linkages between extratropical cyclone (ETC) properties and impacts on evaporation and precipitation in the GLR, we use an ETC impacts dataset derived from the NCEP Climate Forecast System Reanalysis (CFSR) (Saha et al., 2010), which has a horizontal resolution of $0.5° \times 0.5°$ and assimilates a wide range of observations.

ETCs are identified and tracked over 1979–2019 using the Crawford and Serreze (CS) detection algorithm applied to mean sea level pressure (MSLP) (Crawford & Serreze, 2016; Crawford et al., 2021). We retain storms that enter the GLR (38–52°N, 72–96°W; Figure 1). To isolate synoptic-scale systems, we require a minimum radial pressure difference of 7.5 hPa and a radius of at least 250 km at one or more timesteps. Storm radius is defined using the outermost closed pressure isobar, with the maximum taken over the storm lifetime. The resulting dataset includes 3317 ETCs sampled at six-hourly resolution.

We extract precipitation (P) and evaporation (E, derived from latent heat flux and surface temperature) for each storm. Impacts are computed over a window from 24 hours prior to GLR entry to 48 hours after exit, centered on minimum MSLP. We analyze storm-integrated P and E, with evaporation expressed as an anomaly relative to a 1981–2000 climatology. Lake-wide averages are computed using latitude-weighted means.

We characterize storm evolution using event-level metrics derived from the CFSR-based ETC inventory. Storm structure is represented by minimum central pressure, maximum pressure gradient, maximum radius, and maximum propagation speed, each evaluated over the storm lifetime. Interaction with the lake system is quantified as the fraction of each storm's lifetime spent within the GLR.

To represent storm life cycle stage at lake interaction, we define a maturity proxy as the fraction of storm lifetime elapsed at first GLR entry:

$$M = \frac{t_{\text{entry}} - t_{\text{genesis}}}{t_{\text{lysis}} - t_{\text{genesis}}} \tag{1}$$

where t_{genesis}, t_{entry}, and t_{lysis} denote the times of cyclogenesis, first GLR entry, and dissipation. Larger values indicate storms that enter later in their evolution.

This metric does not fully describe storm structure or evolution but provides a consistent measure across events, allowing us to test whether storm maturity and GLR residence time organize differences in extreme precipitation and evaporation risk.

3 Methods

In this section, we describe the unsupervised classification framework used to identify distinct classes of extratropical cyclones (3.1), along with the definition of extremes and the probabilistic metrics used to assess relative impact risk (3.2).

3.1 Unsupervised classification as a hypothesis generator

We use unsupervised classification to identify covariance structure between storm properties and lake interactions without imposing *a priori* assumptions. Such approaches are well suited to complex Earth system problems, where structure emerges from combinations of variables rather than single thresholds (Sonnewald et al., 2019, 2020, 2023; Maze et al., 2017; Jones & Ito, 2019; Jones et al., 2019, 2023).

We apply Gaussian mixture modeling (GMM), which represents the joint distribution of storm characteristics as a weighted sum of multivariate Gaussian components and provides probabilistic assignment of events to classes. The feature space is constructed from event-level storm properties and interaction metrics summarizing storm intensity, structure, and evolution (Section 2), providing a compact and physically interpretable representation for classification.

We evaluate GMMs with varying numbers of components using model selection metrics that balance goodness of fit and parsimony (Supporting Information). Solutions with 2–4 components are defensible, but the final choice must be guided by the scientific objective (Rosso et al., 2020; Jones et al., 2023). We therefore select a two-class solution based on interpretability, physical coherence, and robustness across sensitivity tests (Supporting Information). Similar parsimonious approaches have been used to distinguish large-scale ocean structure in the North Atlantic (Desbruyères et al., 2021).

Our emphasis on a simple classification reflects the use of unsupervised modeling as a hypothesis generator rather than a definitive taxonomy (Kaiser et al., 2022). Higher-order structure may be present, but the two-class framework provides a clear basis for assessing differences in extreme precipitation and evaporation risk without overfitting or obscuring physical interpretation.

3.2 Definition of extremes and risk metrics

We define extreme precipitation and evaporation events using percentile-based thresholds computed separately for each lake and season. For precipitation, we define extremes

as events exceeding the 95th percentile of storm-associated lake-mean overlake precipitation from the entire 1979–2019 period in the CSFR. For evaporation, we define extremes using the lower 5th percentile of evaporation anomalies, corresponding to the most negative (i.e. strongest upward) lake–atmosphere moisture flux events. This approach accounts for strong seasonal variability while avoiding assumptions about the underlying distribution of impacts. We quantify differences in extreme-event likelihood between storm classes using probabilistic risk metrics, including the risk ratio (RR) and risk difference (RD), which compare the probability of exceeding a given threshold conditional on storm class membership (Class 1 and Class 2):

$$\mathrm{RR} = \frac{P(\text{Extreme} \mid \text{Class 2})}{P(\text{Extreme} \mid \text{Class 1})} \tag{2}$$

$$\mathrm{RD} = P(\text{Extreme} \mid \text{Class 2}) - P(\text{Extreme} \mid \text{Class 1}) \tag{3}$$

These metrics quantify probabilistic differences in impact risk conditional on storm class membership, as opposed to deterministic attribution. To assess uncertainty in these estimates, we use nonparametric bootstrap resampling. Confidence intervals are computed by repeatedly resampling storms with replacement and recalculating the risk metrics across bootstrap realizations. This framework emphasizes probabilistic interpretation and robustness rather than deterministic attribution, and supports comparisons across lakes, seasons, and storm classes.

4 Results from a two-class model

Gaussian mixture modeling identifies two distinct classes of extratropical cyclones affecting the GLR (Figure 2), which differ systematically across multiple storm properties related to intensity, structure, and evolution. Type 1 storms tend to exhibit lower minimum central pressures overall, with a distribution that includes a longer tail toward lower central pressures. These storms also show a higher peak at faster maximum propagation speeds and a broader distribution of maximum pressure gradients. In addition, Type 1 storms tend to be larger, with storm radius distributions shifted toward higher values relative to Type 2 storms. The strongest separation between the two classes arises in metrics describing storm evolution and interaction with the Great Lakes. Type 1 storms spend a smaller fraction of their total lifetime within the GLR and are characterized by consistently low values of the maturity proxy, indicating that they enter the region early in their life cycle. In contrast, Type 2 storms typically interact with the Great Lakes later in their evolution and remain in the region for a larger fraction of their lifetime. Together, these differences indicate that the two classes primarily separate storms by when they interact with the Great Lakes system and how long that interaction persists, rather than by a single measure of storm intensity.

For evaporation anomalies, a strong and spatially coherent signal emerges in autumn (SON). Across all five lakes, Type 1 (early–life cycle) storms exhibit a systematically lower likelihood of producing extreme evaporation events than Type 2 (late–life cycle) storms, with risk ratios consistently below unity and positive risk differences across the basin (Fig. 3). Median risk differences range from approximately 4% in Lake Superior to roughly 7% in Lake Ontario, with uncertainty intervals remaining above zero for all lakes. Importantly, these results reflect evaporation anomalies, with the seasonal cycle removed, indicating that the signal does not arise from the climatological dominance of fall evaporation but instead reflects differences in storm characteristics.

In contrast, evaporation extremes in winter (DJF), spring (MAM), and summer (JJA) do not exhibit a robust or spatially consistent dependence on storm class. In these seasons, risk ratios generally span unity and risk differences are indistinguishable from

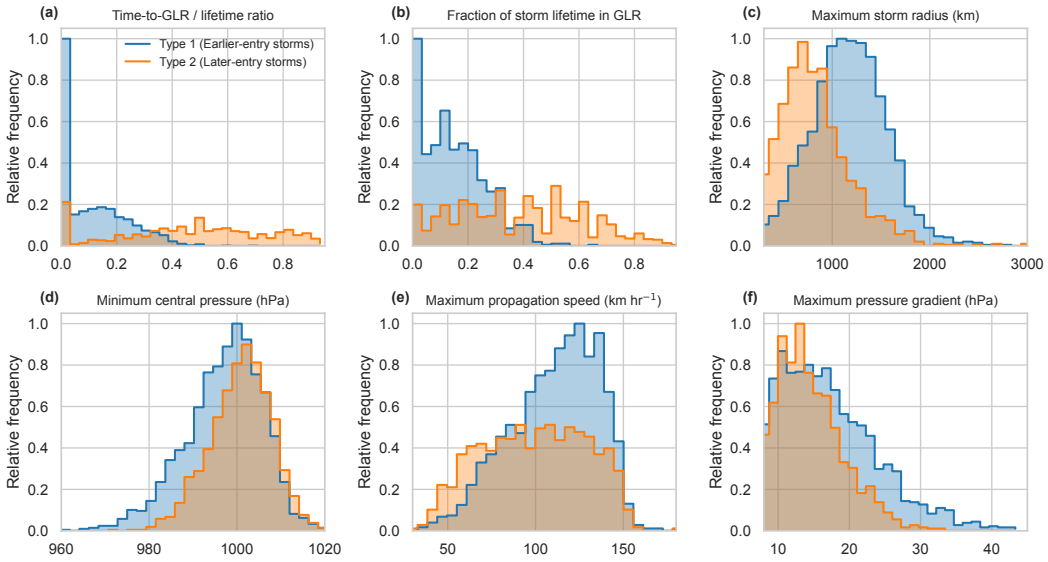

Figure 2. Histograms of storm properties for the two classes: (a) maturity at GLR entry, (b) fraction of storm lifetime in the GLR, and lifetime maxima of (c) storm radius, (d) central pressure (minimum), (e) wind speed, and (f) pressure gradient.

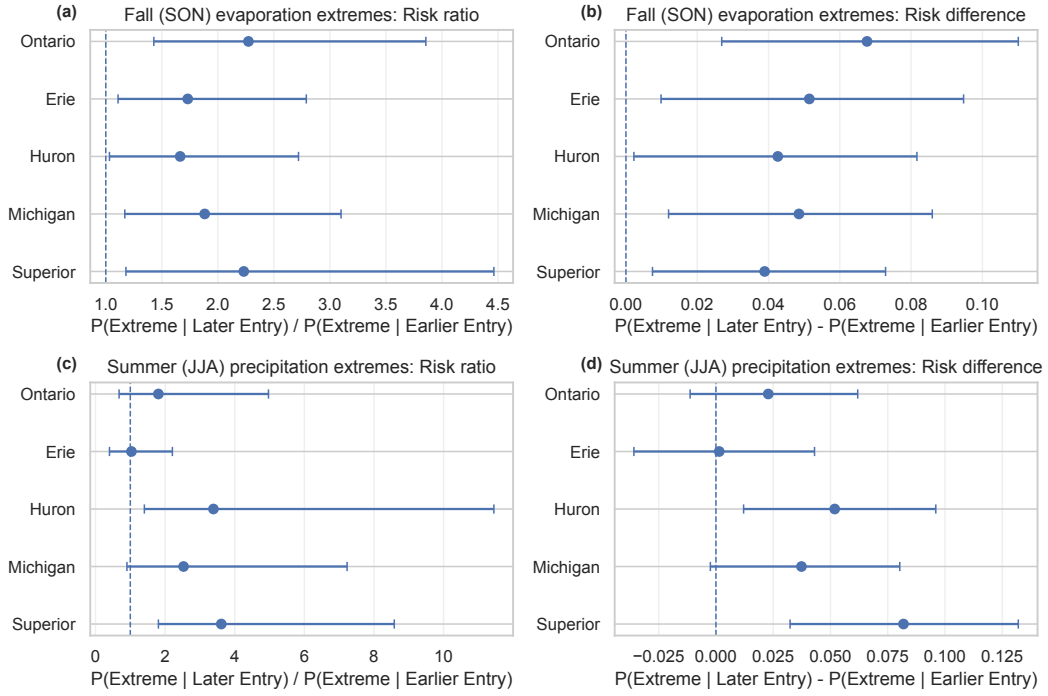

Figure 3. Risk ratios (a, c) and risk differences (b, d) between storm classes for seasons with the strongest signals: evaporation extremes (a, b) in autumn (SON) and precipitation extremes (c, d) in summer (JJA). Points show bootstrap medians; error bars indicate the range of bootstrap estimates. Values greater than 1 (RR) or 0 (RD) indicate elevated risk for later-entry storms.

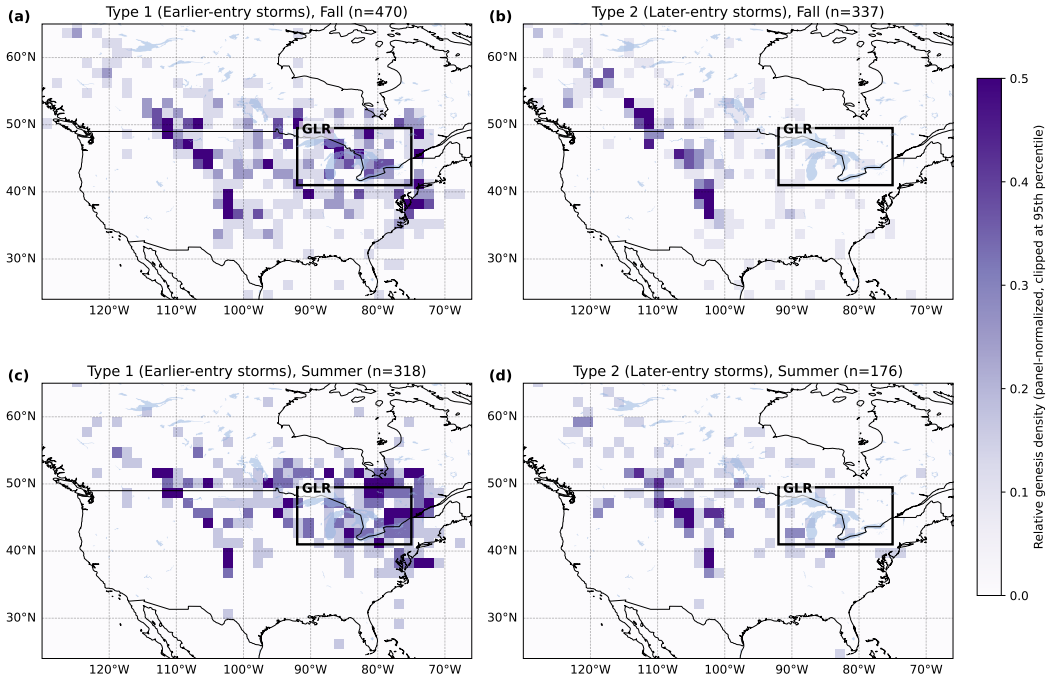

Figure 4. Storm genesis density by class and season. Panels show relative cyclone genesis frequency (panel-normalized and clipped at the 95th percentile) for (a) Type 1 (earlier-entry), autumn (SON), (b) Type 2 (later-entry), autumn (SON), (c) Type 1 (earlier-entry), summer (JJA), and (d) Type 2 (later-entry), summer (JJA).

zero within uncertainty bounds, with only weak and isolated deviations (e.g. in Lake Erie) that lack basin-wide coherence (Supporting Information).

Precipitation extremes also show a seasonally constrained response, albeit with differences between the upper and lower lakes. During summer (JJA), earlier–entry storms are associated with a lower probability of extreme precipitation in the upper Great Lakes (Lakes Superior, Michigan, and Huron), where risk ratios fall below unity and median risk differences remain positive. In contrast, precipitation extremes in Lakes Erie and Ontario during summer show no statistically distinguishable class dependence. Outside of summer, precipitation extremes do not display systematic differences between storm classes across the basin.

Taken together, these results indicate that storm life cycle differences most strongly modulate extreme impacts through autumn evaporation across all lakes and summer precipitation in the upper Great Lakes. Other seasons show comparatively weak or absent class dependence, underscoring the importance of both seasonality and storm evolution in shaping ETC-driven hydroclimate extremes.

The two storm classes also exhibit systematic differences in their geographic origins, as reflected in the spatial distribution of cyclogenesis locations (Figure 4). Late–life cycle storms tend to originate farther west. In contrast, early–life cycle storms display a more diffuse set of origins, spanning a broader range of longitudes and latitudes. This west–east contrast produces a visible imprint of orographic forcing in both classes, with the Rocky Mountains acting as a dominant organizing feature in storm lee cyclogenesis.

However, these origin differences do not by themselves explain the observed differences in extreme precipitation and evaporation risk. Storms from similar genesis regions can produce markedly different impacts upon entering the GLR, depending on their stage of evolution and the duration of their interaction with the lakes. In this sense, storm origin provides useful contextual information but offers limited explanatory power for impact variability when considered in isolation. Instead, storm maturity at Great Lakes entry and residence time within the region provide a more direct and physically relevant framework for interpreting differences in extreme lake–atmosphere fluxes.

5 Discussion

This study examined how extratropical cyclone life cycle evolution relates to extreme precipitation and evaporation in the Great Lakes. Using a storm-centric framework, we identified two classes that differ in maturity at Great Lakes entry and in the fraction of storm lifetime spent within the basin. These differences correspond to consistent probabilistic shifts in extreme impact risk, particularly for evaporation and, more selectively, precipitation. The results describe shifts in risk rather than deterministic outcomes and show that storm evolution provides a useful organizing axis for lake–atmosphere interactions.

Strong autumn evaporation from the Great Lakes is well established and linked to large air–lake temperature contrasts and synoptic forcing associated with extratropical cyclones (Lofgren & Zhu, 2000; Notaro et al., 2013; Hunter et al., 2015; Anderson & Gronewold, 2025; Laird & Kristovich, 2002; Polderman & Pryor, 2004). Here we show that these extremes are modulated by storm evolution: storms entering later in their life cycle exhibit higher risk of extreme evaporation across all lakes. This signal persists after removing the seasonal cycle, indicating a storm-dependent modulation of lake–atmosphere fluxes.

Maturity at Great Lakes entry serves as a compact descriptor of storm structure at interaction. Storms entering later in their life cycle are more likely to exhibit a well-developed cold sector, broader wind field, and more spatially coherent circulation, all of which can enhance and sustain basin-scale air–lake fluxes. Their greater fraction of lifetime within the GLR is consistent with this interpretation, reflecting both timing of interaction and persistence of favorable conditions. While not a complete dynamical description, this metric organizes the degree to which storms impose sustained forcing on the lake system.

These evaporation extremes may influence broader hydroclimate responses. Enhanced turbulent fluxes increase lower-atmospheric moisture, potentially contributing to localized precipitation and downstream lake-effect processes. While not resolved here, this suggests that storm evolution can shape both immediate and integrated basin responses.

In contrast to the basin-wide signal in autumn evaporation, precipitation extremes exhibit a more spatially heterogeneous response to storm class. Differences in precipitation risk emerge most clearly during summer and are largely confined to the upper Great Lakes, with weaker or indistinguishable signals in the lower lakes. This pattern likely reflects seasonal shifts in storm tracks: the northward displacement of baroclinic zones during summer reduces the frequency of ETC impacts on Lake Erie and Lake Ontario. Precipitation extremes arise from processes that vary across lakes and events, including moisture availability, frontal structure, and mesoscale lake–atmosphere interactions. Storm maturity may still organize the large-scale dynamical environment, but its influence on precipitation is less direct than for evaporation and is therefore expressed less uniformly. The absence of a basin-wide precipitation signal should not be interpreted as evidence of fundamentally different physical pathways.

The two storm classes exhibit systematic differences in geographic origin, as reflected in their cyclogenesis locations. Late–life cycle storms tend to originate farther west, while early–life cycle storms display a broader and more diffuse genesis distribution. These patterns are consistent with established pathways of lee cyclogenesis and midlatitude storm development, leaving a clear imprint of orographic forcing (Zishka & Smith, 1980; Mahdi et al., 2019).

However, geographic origin does not fully explain differences in extreme lake impacts. Storms with similar genesis locations can interact with the Great Lakes at different stages of their evolution, leading to distinct wind structures, residence times, and air–lake fluxes. The results therefore point to storm maturity at Great Lakes entry, rather than origin, as a more informative axis for organizing differences in extreme precipitation and evaporation risk. This reframes storm impacts in terms of storm state at interaction rather than birthplace, providing a more physically grounded perspective on lake–atmosphere coupling.

The finding that earlier-entry storms exhibit larger maximum radii is initially counterintuitive, as these systems are less mature at the time of Great Lakes entry (Figure 2(c)). This reflects the distinction between storm state at entry and the full life cycle. Because the radius metric captures the maximum extent attained over the storm lifetime, storms entering earlier may continue to intensify and expand after interacting with the Great Lakes, ultimately reaching larger sizes than later-entry storms. Early-entry storms therefore represent systems with greater remaining growth potential, while later-entry storms may already be near or past peak structural development. This interpretation is consistent with the broader framework used here, in which classification reflects timing of regional interaction rather than a fixed dynamical stage.

Our storm-centric framing connects to broader efforts to classify extratropical cyclones by dynamical and thermodynamical structure. Cyclogenesis spans a high-dimensional continuum of precursor conditions, reflecting variability in upper-level forcing, baroclinicity, and diabatic processes (Graf et al., 2017). Some identified classes, including those associated with strong baroclinicity and upper-level PV anomalies, tend to originate closer to the Great Lakes and are therefore more likely to enter the region earlier in their life cycle. These systems are also associated with strong upward motion and can advect cold, dry continental air over the lakes, favoring enhanced evaporation. While not diagnosed explicitly here, these connections are consistent with the interpretation that storm evolution and air-mass structure jointly influence evaporation risk.

In contrast, the maturity metric used here reduces this complexity to a single time-based descriptor. Despite this simplification, maturity at GLR entry provides a useful organizing axis for hydroclimate impacts, particularly for autumn evaporation extremes.

One limitation is the representation of local-scale processes embedded within ETCs. Features on scales smaller than about 10 km can strongly modulate precipitation, particularly through lake–atmosphere interactions. In coarse-resolution reanalyses such as CFSR, these processes are only partially resolved or parameterized. This is especially relevant for mechanisms such as lake-effect snowfall and lake-enhanced precipitation, which can produce spatial heterogeneity in impacts. The precipitation signals attributed to each storm type should therefore be interpreted as large-scale tendencies rather than localized extremes.

Another limitation is the simplicity of the maturity proxy used to characterize storm evolution at Great Lakes entry. This metric collapses a complex, multivariate life cycle into a single scalar quantity. We adopt this simplification to preserve objectivity, scalability, and reproducibility across several thousand events. More detailed, physically grounded definitions of storm maturity that can be applied consistently across long reanalysis records remain an open challenge.

Despite its simplicity, the maturity proxy captures physically meaningful structure in the ETC population and yields coherent, interpretable differences in extreme impact risk. The resulting storm classes align with expected distinctions in storm evolution and lake interaction, revealing systematic relationships between storm state, residence time, and extreme impacts that are not apparent from seasonality or storm origin. We therefore view this proxy as a first-order diagnostic that enables discovery within a storm-centric framework rather than a definitive measure of storm maturity. Future work can refine these diagnostics while retaining the core insight that storm evolution at lake interaction plays a central role in shaping extreme impacts.

The storm-centric framework presented here is transferable to other large lake systems, inland seas, and coastal regions influenced by extratropical cyclones. Its core elements, including objective storm tracking, unsupervised classification, and probabilistic risk metrics, are not specific to the Great Lakes and can be applied wherever storm-resolved impact datasets are available. By accounting for storm evolution and residence time, this framework enables more granular assessments of extreme impact risk than approaches based solely on seasonality, storm counts, or geographic origin, without implying deterministic attribution or forecast skill.

The strong association between storm maturity and extreme evaporation highlights the importance of storm evolution for lake–atmosphere coupling and downstream impacts such as lake-effect precipitation, which can be consequential on event timescales. While the specific thresholds, proxies, and impact definitions used here reflect the Great Lakes system, these components can be adapted to other regions while retaining the storm-centric perspective.

Future work can refine the representation of storm evolution while retaining a storm-centric perspective. More detailed maturity diagnostics, including frontal structure, moisture transport pathways, or dynamically defined life cycle markers, could augment or replace the simple proxy used here. Coupling storm-resolved classifications with moisture source diagnostics or process-based air–lake flux models may further clarify the mechanisms linking storm evolution to extreme impacts. While this study does not assess forecast skill, integrating storm-centric classifications into forecasting contexts represents a potential direction for evaluating whether storm evolution can improve probabilistic assessments of extreme lake–atmosphere interactions and their impacts.

This study shows that extreme hydroclimate impacts in large lake regions depend not only on when storms occur or where they originate, but on how they evolve during lake interaction. By distinguishing extratropical cyclones based on life cycle stage and residence time within the GLR, we show that storm evolution provides a physically meaningful axis for organizing differences in extreme precipitation and evaporation risk. Accounting for storm maturity clarifies why certain storms are more likely to produce extreme lake–atmosphere fluxes, offering a storm-centric perspective that complements seasonal and climatological analyses without overextending their scope.

Open Research Section

Code and data used in this analysis are archived and publicly available (Jones et al., 2026).

Inclusion in Global Research Statement

This study uses publicly available reanalysis and derived datasets and does not involve fieldwork, local communities, or region-specific research partnerships. As such, no additional inclusion or permitting considerations apply.

Conflict of Interest declaration

The authors declare there are no conflicts of interest for this manuscript.

Acknowledgments

This study was funded by the National Oceanic and Atmospheric Administration (NOAA) through awards to the Cooperative Institute for Great Lakes Research (CIGLR) under the NOAA Cooperative Agreement with the University of Michigan (NA22OAR4320150) and the Infrastructure Investment and Jobs Act award NA23OAR4050594. The authors used generative AI tools (ChatGPT, OpenAI; GPT-5.3) to assist with manuscript editing and limited code development, with the goal of improving clarity, structure, and reproducibility. All scientific content, analysis, and interpretation were developed and verified by the authors, who take full responsibility for the work. We thank Bryan Mroczka for help with the dataset creation. This is CIGLR contribution XXXX and NOAA GLERL contribution XXXX. Author L. Ru was supported by the University of Michigan Undergraduate Research Opportunity Program (UROP).

References

Agustí-Panareda, A., Gray, S. L., Craig, G. C., & Thorncroft, C. (2005, June). The Extratropical Transition of Tropical Cyclone Lili (1996) and Its Crucial Contribution to a Moderate Extratropical Development. *Monthly Weather Review*, *133*(6), 1562–1573. doi: 10.1175/MWR2935.1

Anderson, E. J., & Gronewold, A. D. (2025). Does Ice Cover Cap Evaporation in Large Lakes? *Geophysical Research Letters*, *52*(19), e2025GL117112. doi: 10.1029/2025GL117112

Angel, J. R., & Isard, S. A. (1997, September). An Observational Study of the Influence of the Great Lakes on the Speed and Intensity of Passing Cyclones. *Monthly Weather Review*.

Angel, J. R., & Isard, S. A. (1998, January). The Frequency and Intensity of Great Lake Cyclones. *Journal of Climate*.

Angel, J. R., & Kunkel, K. E. (2010, January). The response of Great Lakes water levels to future climate scenarios with an emphasis on Lake Michigan-Huron. *Journal of Great Lakes Research*, *36*, 51–58. doi: 10.1016/j.jglr.2009.09.006

Anyah, R. O., & Semazzi, F. (2009). Idealized simulation of hydrodynamic characteristics of Lake Victoria that potentially modulate regional climate. *International Journal of Climatology*, *29*(7), 971–981. doi: 10.1002/joc.1795

Booth, J. F., Naud, C. M., & Jeyaratnam, J. (2018). Extratropical Cyclone Precipitation Life Cycles: A Satellite-Based Analysis. *Geophysical Research Letters*, *45*(16), 8647–8654. doi: 10.1029/2018GL078977

Chang, E. K. M., Ma, C.-G., Zheng, C., & Yau, A. M. W. (2016). Observed and projected decrease in Northern Hemisphere extratropical cyclone activity in summer and its impacts on maximum temperature. *Geophysical Research Letters*, *43*(5), 2200–2208. doi: 10.1002/2016GL068172

Clare, R. M., Desai, A. R., Martin, J. E., Notaro, M., & Vavrus, S. J. (2023, April). Extratropical Cyclone Response to Projected Reductions in Snow Extent over the Great Plains. *Atmosphere*, *14*(5), 783. doi: 10.3390/atmos14050783

Crawford, A. D., Schreiber, E. A. P., Sommer, N., Serreze, M. C., Stroeve, J. C., & Barber, D. G. (2021, August). Sensitivity of Northern Hemisphere Cyclone Detection and Tracking Results to Fine Spatial and Temporal Resolution Using ERA5. *Monthly Weather Review*. doi: 10.1175/MWR-D-20-0417.1

Crawford, A. D., & Serreze, M. C. (2016, July). Does the Summer Arctic Frontal Zone Influence Arctic Ocean Cyclone Activity? *Journal of Climate*, *29*(13), 4977–4993. doi: 10.1175/JCLI-D-15-0755.1

Desbruyères, D., Chafik, L., & Maze, G. (2021, February). A shift in the ocean circulation has warmed the subpolar North Atlantic Ocean since 2016. *Communications Earth & Environment*, *2*(1), 48. doi: 10.1038/s43247-021-00120-y

Eichler, T., & Higgins, W. (2006, May). Climatology and ENSO-Related Variability of North American Extratropical Cyclone Activity. *Journal of Climate*. doi: 10.1175/JCLI3725.1

Fritzen, R., Lang, V., & Gensini, V. A. (2021, September). Trends and Variability of North American Cool-Season Extratropical Cyclones: 1979–2019. *Journal of Applied Meteorology and Climatology*. doi: 10.1175/JAMC-D-20-0276.1

Gertler, C. G., & O'Gorman, P. A. (2019, March). Changing available energy for extratropical cyclones and associated convection in Northern Hemisphere summer. *Proceedings of the National Academy of Sciences*, *116*(10), 4105–4110. doi: 10.1073/pnas.1812312116

Graf, M. A., Wernli, H., & Sprenger, M. (2017). Objective classification of extratropical cyclogenesis. *Quarterly Journal of the Royal Meteorological Society*, *143*(703), 1047–1061. doi: 10.1002/qj.2989

Gronewold, A. D., Bruxer, J., Durnford, D., Smith, J. P., Clites, A. H., Seglenieks, F., ... Fortin, V. (2016). Hydrological drivers of record-setting water level rise on Earth's largest lake system. *Water Resources Research*, *52*(5), 4026–4042. doi: 10.1002/2015WR018209

Hanrahan, J., Langlois, J., Cornell, L., Huang, H., Winter, J. M., Clemins, P. J., ... Bruyère, C. (2021, July). Examining the Impacts of Great Lakes Temperature Perturbations on Simulated Precipitation in the Northeastern United States. *Journal of Applied Meteorology and Climatology*. doi: 10.1175/JAMC-D-20-0169.1

Hanrahan, J. L., Kravtsov, S. V., & Roebber, P. J. (2010). Connecting past and present climate variability to the water levels of Lakes Michigan and Huron. *Geophysical Research Letters*, *37*(1). doi: 10.1029/2009GL041707

Hawcroft, M. K., Shaffrey, L. C., Hodges, K. I., & Dacre, H. F. (2012). How much Northern Hemisphere precipitation is associated with extratropical cyclones? *Geophysical Research Letters*, *39*(24). doi: 10.1029/2012GL053866

Hunter, T. S., Clites, A. H., Campbell, K. B., & Gronewold, A. D. (2015, March). Development and application of a North American Great Lakes hydrometeorological database — Part I: Precipitation, evaporation, runoff, and air temperature. *Journal of Great Lakes Research*, *41*(1), 65–77. doi: 10.1016/j.jglr.2014.12.006

Hutson, A., Fujisaki-Manome, A., & Glassman, R. (2024). Historical Trends in Cold-Season Mid-Latitude Cyclones in the Great Lakes Region. *Geophysical Research Letters*, *51*(16), e2024GL109890. doi: 10.1029/2024GL109890

Jones, D. C., Holt, H. J., Meijers, A. J. S., & Shuckburgh, E. (2019). Unsupervised Clustering of Southern Ocean Argo Float Temperature Profiles. *Journal of Geophysical Research: Oceans*, *124*(1), 390–402. doi: 10.1029/2018JC014629

Jones, D. C., & Ito, T. (2019). Gaussian mixture modeling describes the geography of the surface ocean carbon budget. *Climate Informatics*.

Jones, D. C., Sonnewald, M., Zhou, S., Hausmann, U., Meijers, A. J. S., Rosso, I., ... Naveira Garabato, A. C. (2023, June). Unsupervised classification identifies coherent thermohaline structures in the Weddell Gyre region. *Ocean Science*, *19*(3), 857–885. doi: 10.5194/os-19-857-2023

Jones, D. C., Ward, J., & Mroczka, B. (2026). *Etc impacts in the great lakes: code and data for storm classification and impact analysis.* Zenodo. Retrieved from `https://doi.org/10.5281/zenodo.19559386` (Zenodo dataset and code release) doi: 10.5281/zenodo.19559386

Kaiser, B. E., Saenz, J. A., Sonnewald, M., & Livescu, D. (2022, November). Automated identification of dominant physical processes. *Engineering Applications of Artificial Intelligence*, *116*, 105496. doi: 10.1016/j.engappai.2022.105496

Kunkel, K. E., Yin, X., Sun, L., Champion, S. M., Stevens, L. E., & Johnson, K. M. (2022, May). Extreme Precipitation Trends and Meteorological Causes Over the Laurentian Great Lakes. *Frontiers in Water*, *4*. doi: 10.3389/frwa.2022.804799

Laird, N. F., & Kristovich, D. A. R. (2002, February). Variations of Sensible and Latent Heat Fluxes from a Great Lakes Buoy and Associated Synoptic Weather Patterns. *Journal of Hydrometeorology*.

Lofgren, B. M., & Zhu, Y. (2000, January). Surface Energy Fluxes on the Great Lakes Based on Satellite-Observed Surface Temperatures 1992 to 1995. *Journal of Great Lakes Research*, *26*(3), 305–314. doi: 10.1016/S0380-1330(00)70694-0

Mahdi, T.-F., Jain, G., Patel, S., & Sidhu, A. K. (2019, August). A review of cyclone track shifts over the Great Lakes of North America: Implications for storm surges. *Natural Hazards*, *98*(1), 119–135. doi: 10.1007/s11069-018-3429-2

Maze, G., Mercier, H., Fablet, R., Tandeo, P., Lopez Radcenco, M., Lenca, P., ... Le Goff, C. (2017, February). Coherent heat patterns revealed by unsupervised classification of Argo temperature profiles in the North Atlantic Ocean. *Progress in Oceanography*, *151*, 275–292. doi: 10.1016/j.pocean.2016.12.008

Neff, B. P., & Nicholas, J. (2005). *Uncertainty in the Great Lakes Water Balance* (Scientific Investigations Report No. 2004-5100). U.S. Geological Survey.

Notaro, M., Holman, K., Zarrin, A., Fluck, E., Vavrus, S., & Bennington, V. (2013, February). Influence of the Laurentian Great Lakes on Regional Climate. *Journal of Climate*, *26*(3), 789–804. doi: 10.1175/JCLI-D-12-00140.1

Pfahl, S., & Wernli, H. (2012, October). Quantifying the Relevance of Cyclones for Precipitation Extremes. *Journal of Climate*, *25*(19), 6770–6780. doi: 10.1175/JCLI-D-11-00705.1

Polderman, N. J., & Pryor, S. C. (2004, January). Linking Synoptic-scale Climate Phenomena to Lake-Level Variability in the Lake Michigan-Huron Basin. *Journal of Great Lakes Research*, *30*(3), 419–434. doi: 10.1016/S0380-1330(04)70359-7

Quinn, F. H. (2009). *Net Basin Supply Comparison Analysis* (Tech. Rep.). Hydroclimate Technical Work Group Task 2.2, St. Clair River Task Team, International Upper Great Lakes Study.

Raible, C. C., Pinto, J. G., Ludwig, P., & Messmer, M. (2021). A review of past changes in extratropical cyclones in the northern hemisphere and what can be learned for the future. *WIREs Climate Change*, *12*(1), e680. doi: 10.1002/wcc.680

Riemer, M., & Jones, S. C. (2010). The downstream impact of tropical cyclones on a developing baroclinic wave in idealized scenarios of extratropical transition. *Quarterly Journal of the Royal Meteorological Society*, *136*(648), 617–637. doi: 10.1002/qj.605

Rosso, I., Mazloff, M. R., Talley, L. D., Purkey, S. G., Freeman, N. M., & Maze, G. (2020). Water Mass and Biogeochemical Variability in the Kerguelen Sector of the Southern Ocean: A Machine Learning Approach for a Mixing Hot Spot. *Journal of Geophysical Research: Oceans*, *125*(3), e2019JC015877. doi: 10.1029/2019JC015877

Saha, S., Moorthi, S., Pan, H.-L., Wu, X., Wang, J., Nadiga, S., ... Goldberg, M. (2010, August). The NCEP Climate Forecast System Reanalysis. *Bulletin of the American Meteorological Society*. doi: 10.1175/2010BAMS3001.1

Scott, R. W., & Huff, F. A. (1996, January). Impacts of the Great Lakes on Regional Climate Conditions. *Journal of Great Lakes Research*, *22*(4), 845–863. doi: 10.1016/S0380-1330(96)71006-7

Sonnewald, M., Dutkiewicz, S., Hill, C., & Forget, G. (2020, May). Elucidating ecological complexity: Unsupervised learning determines global marine eco-

provinces. *Science Advances*, *6*(22), eaay4740. doi: 10.1126/sciadv.aay4740

Sonnewald, M., Reeve, K. A., & Lguensat, R. (2023, May). A Southern Ocean supergyre as a unifying dynamical framework identified by physics-informed machine learning. *Communications Earth & Environment*, *4*(1), 153. doi: 10.1038/s43247-023-00793-7

Sonnewald, M., Wunsch, C., & Heimbach, P. (2019). Unsupervised Learning Reveals Geography of Global Ocean Dynamical Regions. *Earth and Space Science*, *6*(5), 784–794. doi: 10.1029/2018EA000519

Vavrus, S., Notaro, M., & Zarrin, A. (2013, January). The Role of Ice Cover in Heavy Lake-Effect Snowstorms over the Great Lakes Basin as Simulated by RegCM4. *Monthly Weather Review*, *141*(1), 148–165. doi: 10.1175/MWR-D-12-00107.1

Wang, J., Xue, P., Pringle, W., Yang, Z., & Qian, Y. (2022). Impacts of Lake Surface Temperature on the Summer Climate Over the Great Lakes Region. *Journal of Geophysical Research: Atmospheres*, *127*(11), e2021JD036231. doi: 10.1029/2021JD036231

Xiao, C., Lofgren, B. M., & Wang, J. (2018, December). WRF-based assessment of the Great Lakes' impact on cold season synoptic cyclones. *Atmospheric Research*, *214*, 189–203. doi: 10.1016/j.atmosres.2018.07.020

Zishka, K. M., & Smith, P. J. (1980, April). The Climatology of Cyclones and Anticyclones over North America and Surrounding Ocean Environs for January and July, 1950–77. *Monthly Weather Review*.

Supporting Information for "Storm life cycle modulates extreme hydroclimate impact risk: a Great Lakes Region case study"

D. C. Jones[1], J. Ward[2], A. Hutson[1], L. Ru[1],

D. M. Wright[3], A. H. Young[3], L. M. Fry[3]

[1]Cooperative Institute for Great Lakes Research, University of Michigan

[2]US Army Corps of Engineers - Detroit District

[3]NOAA Great Lakes Environmental Research Laboratory

Contents of this file

1. Figures S1 to S6

Introduction

This supporting information provides additional detail on the clustering methodology, robustness of the classification, and supplementary visualizations of storm characteristics and impacts. The figures included here document (i) model selection and clustering diagnostics, (ii) stability of the Gaussian mixture model (GMM) classification, (iii) structure of the feature space, and (iv) seasonal and aggregate impact characteristics.

A parallel ERA5 dataset was processed using the same workflow but is not shown here due to known limitations in ERA5 evaporation estimates over the Great Lakes.

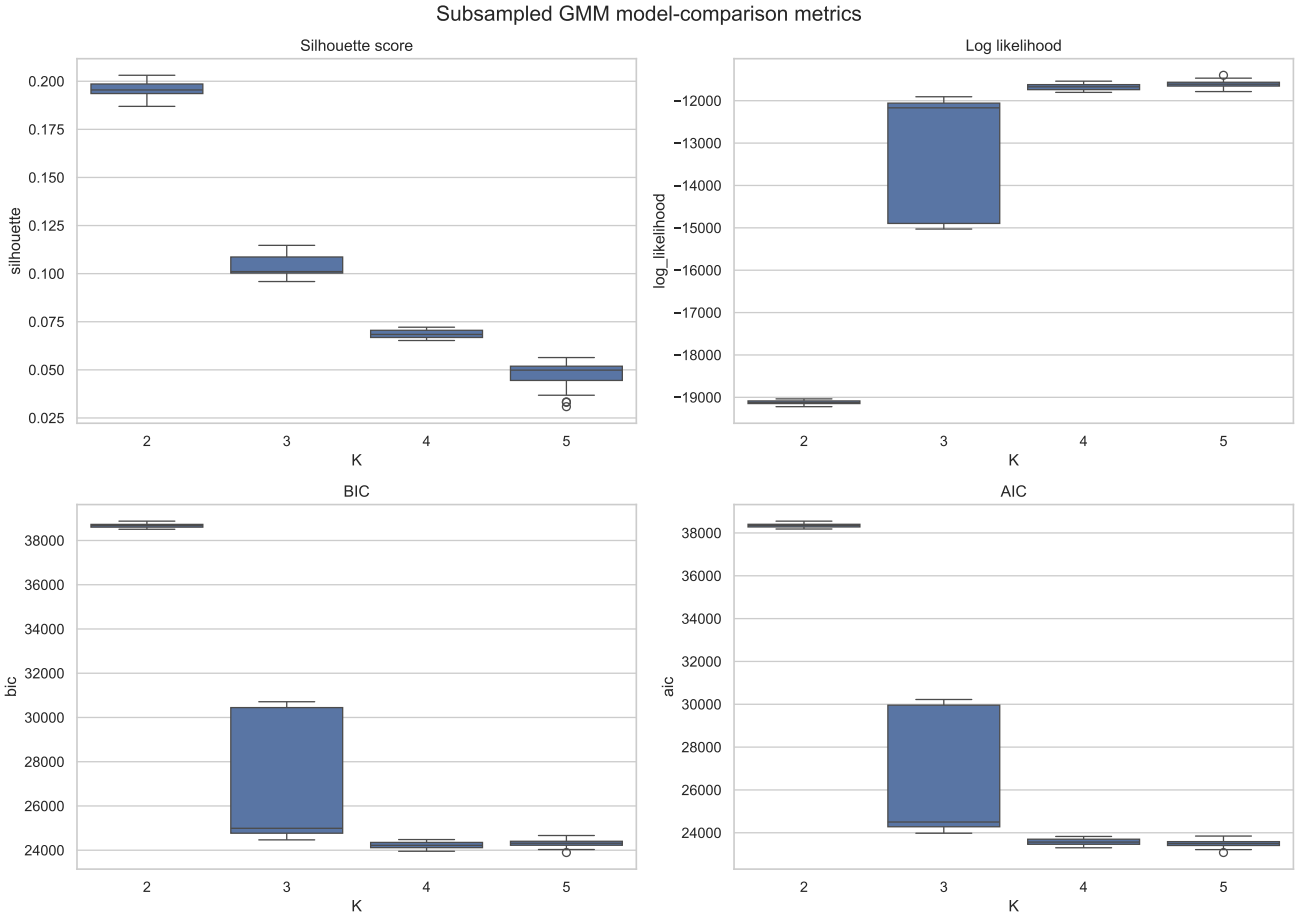

Figure S1. Model selection and clustering diagnostics for Gaussian mixture models with varying numbers of components. Panels show (a) silhouette score, (b) log likelihood, (c) Bayesian Information Criterion (BIC), and (d) Akaike Information Criterion (AIC) across repeated fits. The two-cluster solution (K = 2) provides a balance between model fit and interpretability.

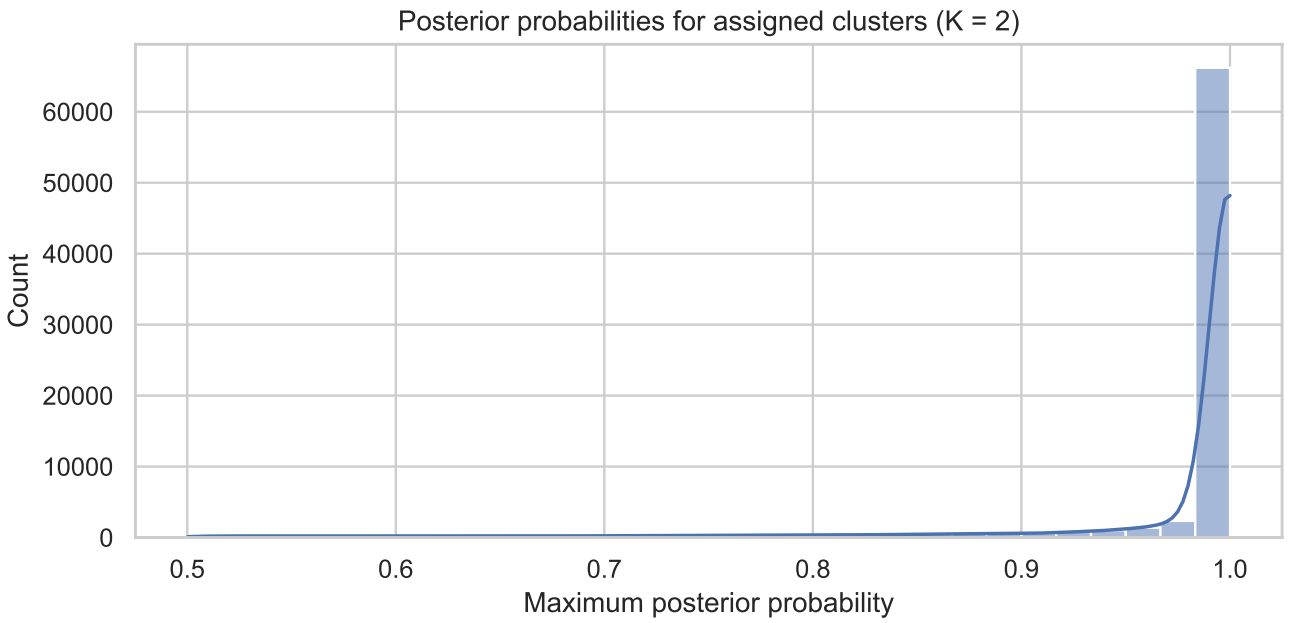

Figure S2. Distribution of maximum posterior probabilities for cluster assignment in the K = 2 model. Most storms are assigned with high confidence (probability near 1), with lower-confidence assignments concentrated near the boundary between clusters.

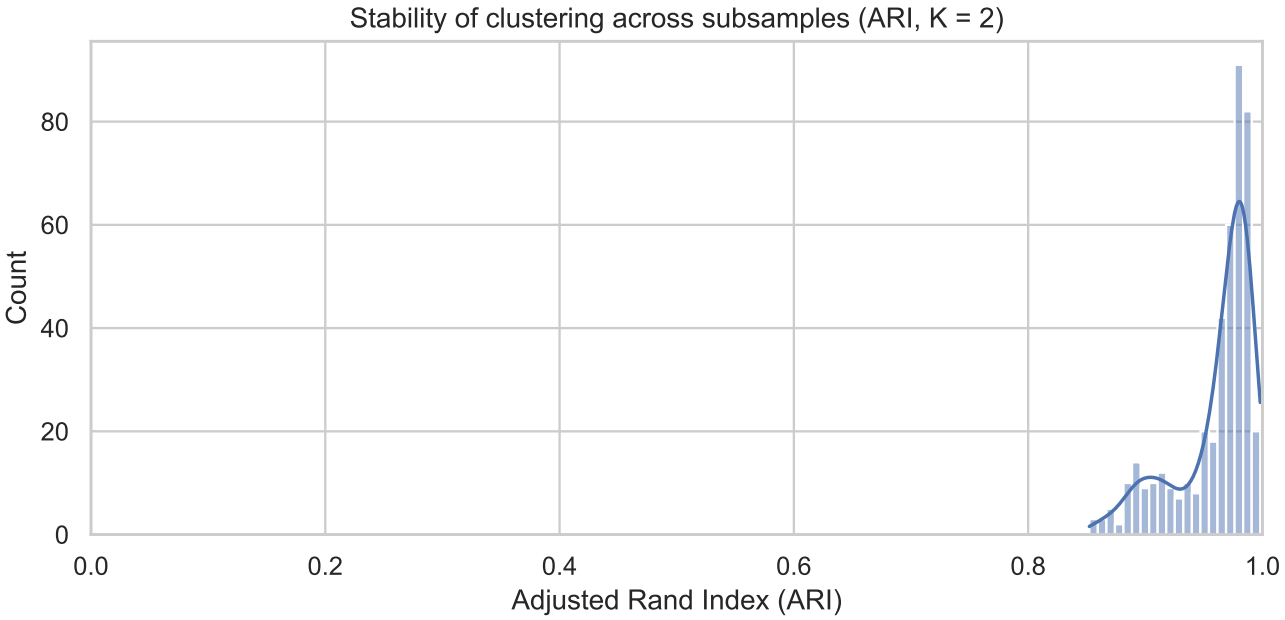

Figure S3. Pairwise adjusted Rand index (ARI) across clustering realizations using repeated subsampling. High ARI values indicate that the clustering is stable to variations in the training subset.

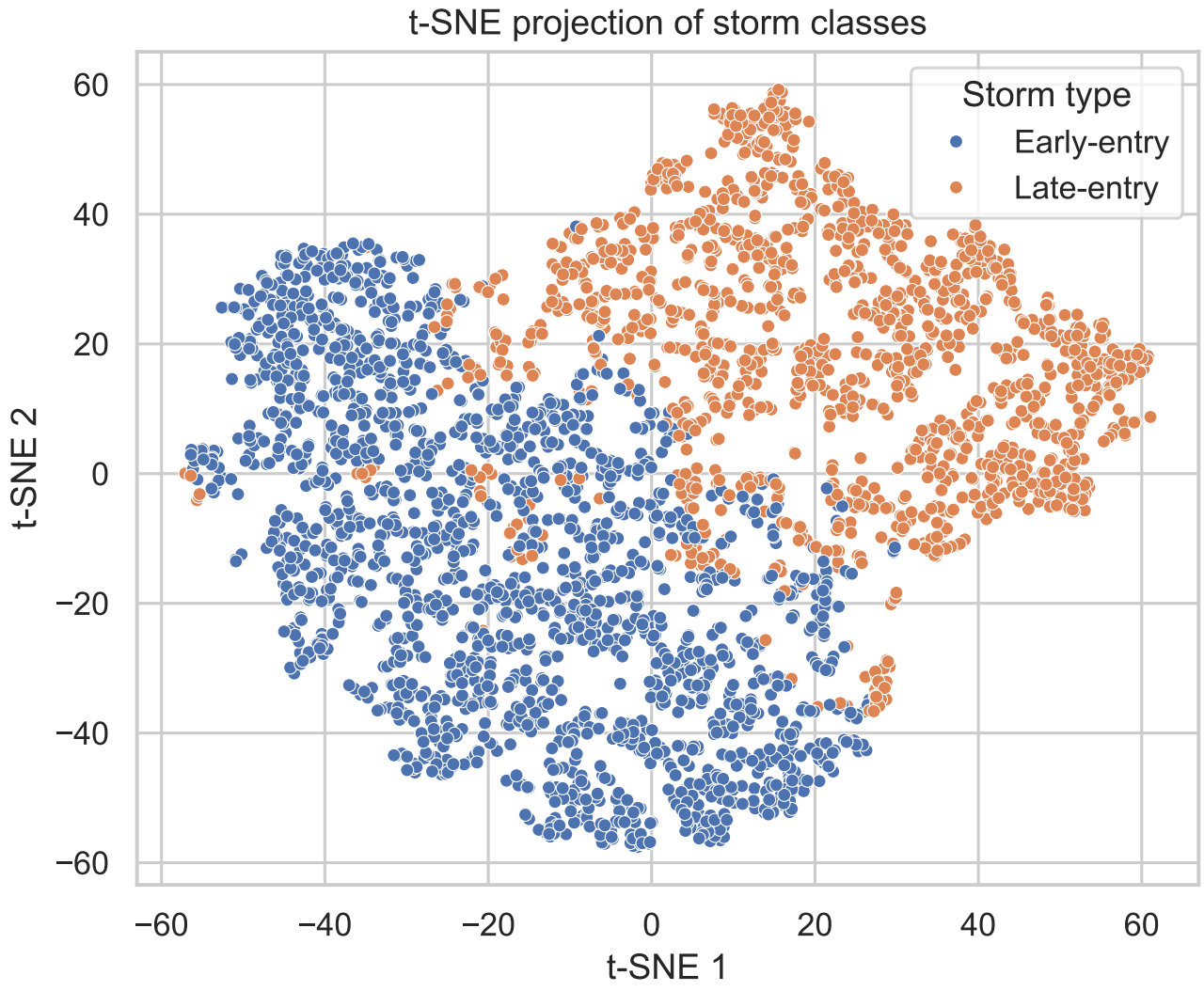

Figure S4. Two-dimensional t-SNE projection of storm features, colored by cluster assignment. The projection illustrates separation between storm types, with some overlap near cluster boundaries. Cluster labels correspond to earlier-entry and later-entry storms as defined in the main text.

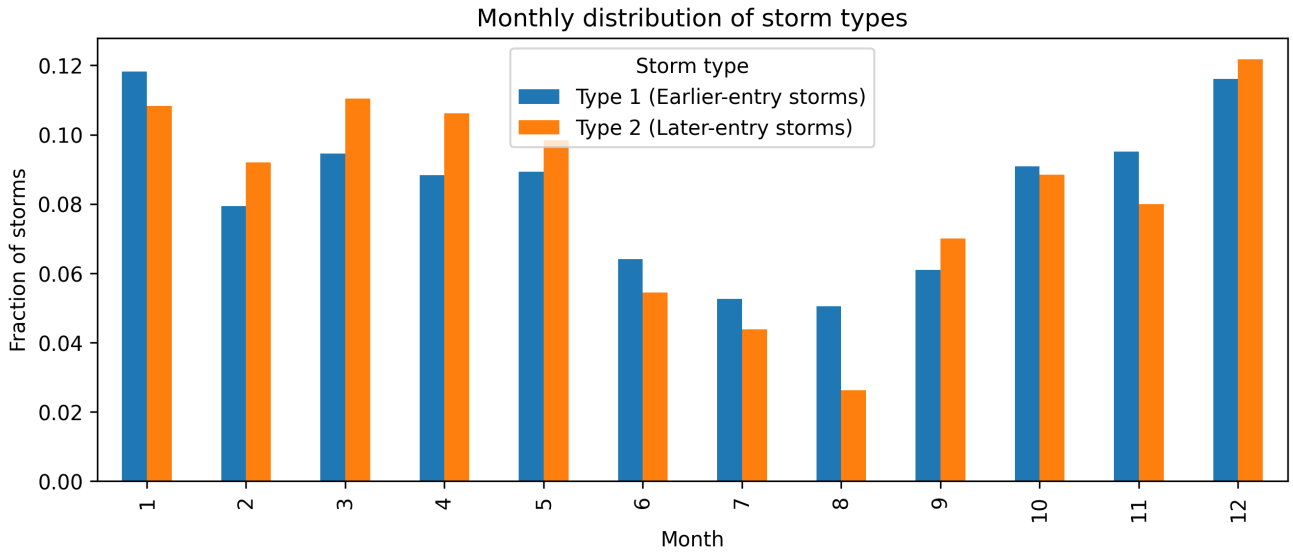

Figure S5. Monthly distribution of storm types, showing the fraction of storms assigned to each cluster by calendar month. Seasonal differences in storm type occurrence are evident.

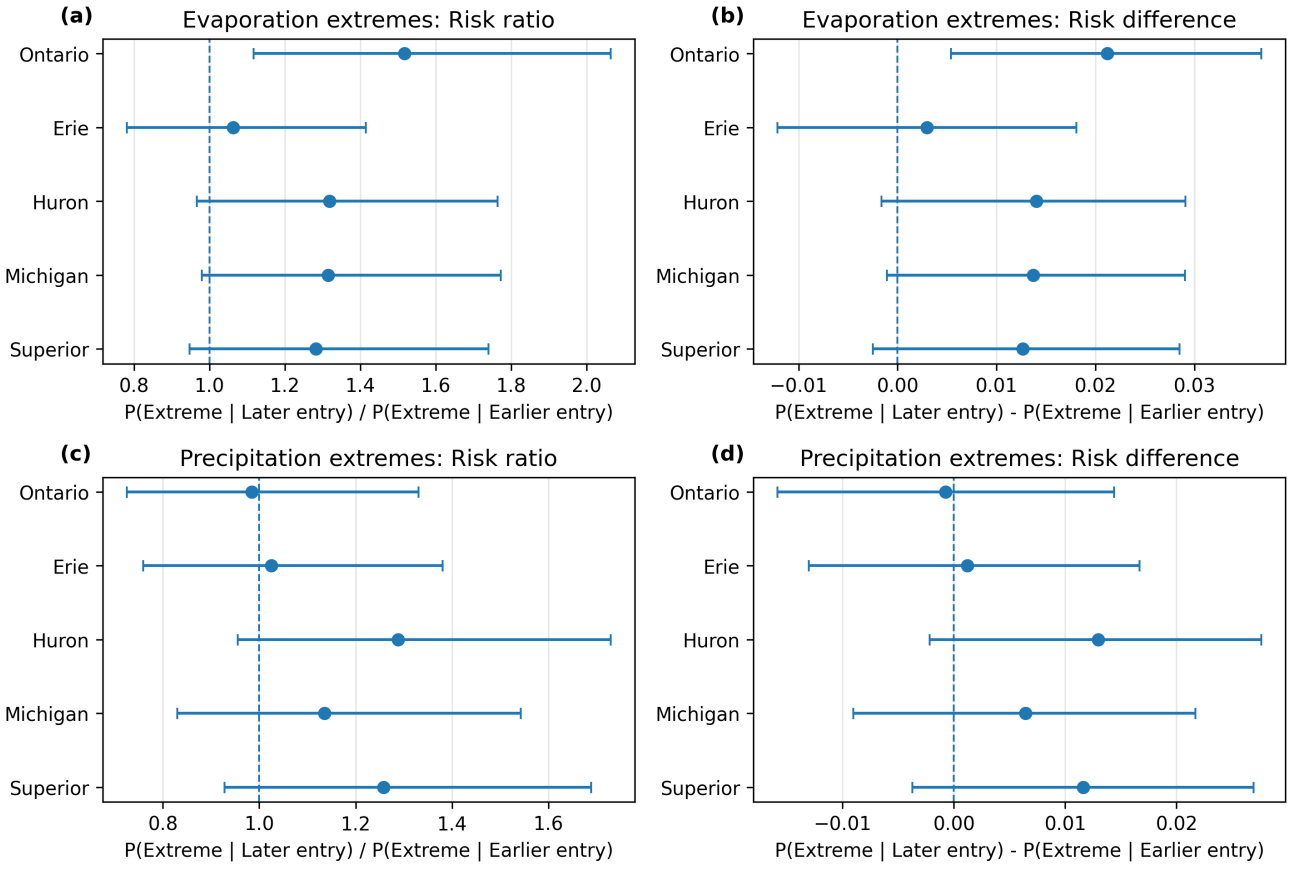

Figure S6. Risk ratio (RR) and risk difference (RD) for evaporation and precipitation extremes across all seasons. Metrics compare the probability of extreme impacts between later-entry and earlier-entry storm types. Error bars represent bootstrap confidence intervals.